Investigation of Mixing Processes in Fluid Flow: Improving MRV Turbulence Quantification and Passive Scalar Distribution Measurements

S.Romig[1], K. John[1], S. Grundmann[1], M. Bruschewski[1]
[1]University of Rostock, Rostock, Germany

Introduction: Mixing processes play a critical role in many industrial flows, such as the blending of air and fuel in gas turbines. Benchmark experiments are conducted in water channels, where key non-dimensional parameters like the Reynolds number ensure similarity to real-world systems. Turbulent mixing is very effective and hence of particular interest. Understanding these mechanisms requires quantitative measurements of the Reynolds stress tensor (RST) for quantifying turbulence and the distribution of a passive scalar. Currently, RST measurements are often compromised by systematic errors, and passive scalar measurements suffer from high noise levels. These limitations hinder the accurate calculation of gradients and derived quantities such as the turbulent Prandtl number, which are essential for deeper analysis.

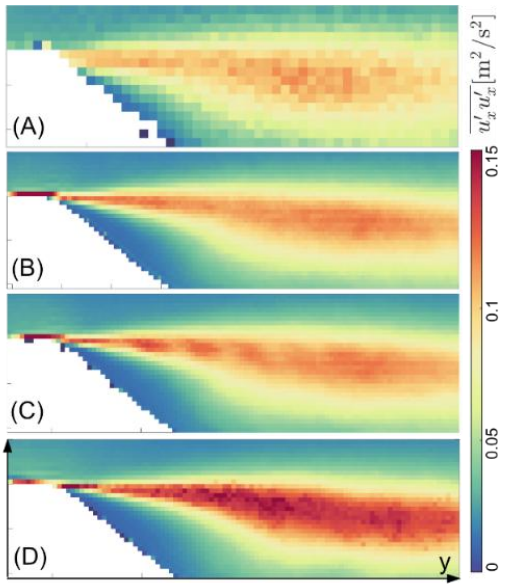

Fig. 1: streamwise RST component from (A) LDV, (B) improved sequence combined readouts, (C) improved sequence, one readout, (D) conventional sequence

This study presents the current progress of a doctoral research project aimed at advancing MRI technology for fluid dynamics applications. The work focuses on enhancing Magnetic Resonance Velocimetry (MRV) pulse sequences to improve RST measurements, as well as refining Magnetic Resonance Contrast (MRC) methods for passive scalar acquisition. The paper concludes with a demonstration of the improved MRV and MRC techniques in a representative experimental setup.

Methods: The current state-of-the-art MRV turbulence quantification is the intravoxel phase dispersion (IVPD) technique [1]. In a phase-contrast gradient recalled echo sequence, the first-order gradient moment M_1 encodes the velocity of the nuclear spins to the signal's phase. Turbulence leads to a velocity distribution producing phase dispersion that results in signal loss. However, the signal's phase also depends on velocity derivatives encoded by higher-order gradient moments. These can lead to overestimating the RST using the IVPD method, as shown in [2]. The idea is to minimize higher-order gradient moments by minimizing TE. Eq. 1 shows the Taylor series of the fluid motion inserted into the signal's phase angle ϕ.

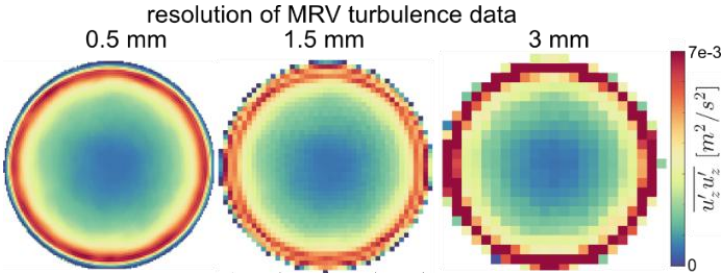

Fig. 2: streamwise RST component acquired with varying resolution

$$\phi = \gamma \int G_x(t)\, x \, dt = \phi_0 + \gamma r_0 \int_{t_0}^{TE} G(t)dt + \gamma u \int_{t_0}^{TE} G(t)t dt + \gamma a \int_{t_0}^{TE} \frac{G(t)t^2}{2} dt + \ldots$$
$$= \phi_0 + \gamma r_0 M_0 + \gamma u M_1 + \frac{\gamma a}{2} M_2 + \cdots \quad \text{Eq. 1}$$

ϕ_0 is the background initial phase, t_0 is the isophase point, when all spins are phase-aligned during excitation, r_0 is the spin's initial position, u its velocity and a its acceleration. It supports the intention of minimizing TE to minimize higher-order gradient moments, as they depend on higher

powers of time. This is achieved via three measures: a high receiver bandwidth and an asymmetric echo shortening the readout gradient, and FAST velocity encoding shortening the velocity encoding process. The low-frequency Gibbs ringing induced by the asymmetric echo is eliminated by applying an inverted readout and combining both partial k-spaces to one whole k-space [3]. Furthermore, previous results indicate that an insufficient voxel size leads to a systematic overestimation of turbulence peak values. Therefore, experiments were conducted with varying spatial resolution in a simple pipe flow and compared to reference data from [4].

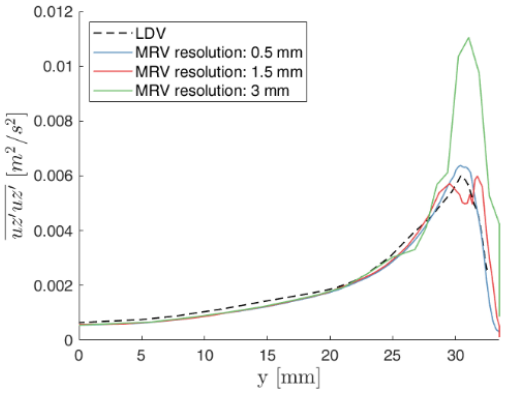

Fig. 3: circumferential average of streamwise RST component acquired with varying resolution compared to LDV data

Results and Discussion: Fig. 1 shows the streamwise component of the RST $\overline{u_x'u_x'}$. The Laser-Doppler-Velocimetry (LDV) reference data (A) and the improved MRV sequence with combined readouts (B) show good agreement, where the sequence without inverted readout shows ringing (C) and the conventional IVPD sequence (D) leads to overestimation of turbulence. The improved sequence reduced the deviation from the LDV data by a factor of 5. The behavior depicted in Fig. 2 and Fig. 3 contrasts with many other fluid mechanic measurement techniques, where low resolution typically results in underestimating peak values due to spatial averaging. Instead, for MRV, overestimation can be observed for lower resolutions. For a resolution of 1.5 mm, even qualitative deviations arise due to an unfavorable choice of resolution, which causes Gibbs ringing in the turbulent peak. The overestimation in MRV arises mainly from mean velocity variations within voxels, which introduce additional intra-voxel phase dispersion. This phenomenon becomes more pronounced as voxel size increases. Correction methods proposed in [4] only apply in case of linear velocity gradients, but for lower resolutions, the gradients are nonlinear here. This suggests that a sufficient resolution is crucial in MRV turbulence quantification. In Fig. 4, a representative benchmark experiment for turbulent mixing [5] with the main channel with cubic obstacles and a jet, where the contrast agent was added, is shown. The top shows the results from the MRC measurements, and the bottom shows the turbulence kinetic energy (TKE $= \frac{1}{2}$ $(\overline{u_x'u_x'} + \overline{u_y'u_y'} + \overline{u_z'u_z'})$), which is often used in fluid mechanics to quantify the amount of turbulence. The MRC quality could be enhanced by exact control of the boundary conditions, which allowed for multiple averages, improving the SNR.

Conclusion:

Improving RST and MRC measurement techniques in generic setups allows for the accurate investigation of mixing processes in more complex industrial applications like gas turbines. This data can hopefully be a basis to validate models for numerical simulations in engineering design processes.

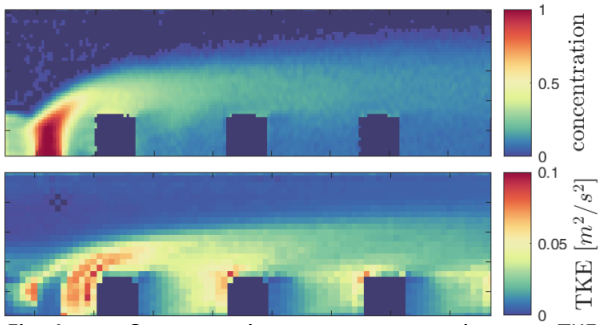

Fig. 4: top: Concentration measurements, bottom: TKE measurements

References: [1] Dyverfeldt, Magn. Reson. Imaging (2009). doi:10.1016/j.mri.2009.05.004; [2] Schmidt, Exp. Fluids (2021). doi:10.1007/s00348-021-03218-3; [3] Romig, Magn. Reson. Imaging (2025). doi:10.1016/j.mri.2025.110333; [4] den Toonder, Phys. Fluids (1997). doi: 10.1063/1.869451; [5] Benson, Exp. Fluids (2023). doi: 10.1007/s00348-023-03572-4.